Development of a New Synthetic Method Based on *In Situ* Strategies for Polyethylene/Clay Composites

Alicia Carrero,[1] Rafael van Grieken,[2] Inmaculada Suarez,[1] Beatriz Paredes[2]

[1]*Department of Chemical and Energy Technology, ESCET, Universidad Rey Juan Carlos, c/ Tulipan s/n, 28933 Mostoles, Madrid, Spain*
[2]*Department of Chemical and Environmental Technology, ESCET, Universidad Rey Juan Carlos, c/ Tulipan s/n, 28933 Mostoles, Madrid, Spain*

Received 13 September 2011; accepted 17 January 2012
DOI 10.1002/app.36830
Published online in Wiley Online Library (wileyonlinelibrary.com).

ABSTRACT: Methods to make polymer composites comprise melt and solution blending, but in the particular case of polyolefins they are not appropriate due to the weak interfacial adhesion. In the present work, *in situ* blended (ISB) together with *in situ* polymerization (ISP) processes have been employed and compared using MAO/$(n\text{BuCp})_2ZrCl_2$ as catalytic system and sepiolite clay as additive in ethylene polymerization. A new method as a combination of the previous ones (ISB + ISP) has been developed and applied to the synthesis of linear low-density polyethylene (LLDPE). When ISB + ISP method is employed high catalytic activities are observed and this combination allows to increase the storage modulus at 25°C up to 26% with 2.8 wt % of clay in LLDPE when silica is employed as catalyst carrier; in that way, copolymer particles with good morphology with higher storage modulus are obtained, useful properties for their use in specific applications. © 2012 Wiley Periodicals, Inc. J Appl Polym Sci 000: 000–000, 2012

Key words: clay; metallocene catalysts; mechanical properties; polyethylene; synthesis

INTRODUCTION

Polyolefin composites are a subset of polymer composites that emerged as a result of the need to meet application requirements not satisfied by synthesized neat polyolefins.[1] In comparison to other polymer composites, polyolefin composites have distinct advantages of lower density, lower cost, easy processing, and good combination of chemical, physical, and mechanical properties.[2,3]

Polyolefin composites may be defined as polyolefin-based materials containing at least one functional nonpolymeric additive of organic or inorganic origin. Additives of interest in the formulation of polyolefin composites include, but not limited to, the following: glass fibers, hollow glass bubbles, clay minerals, carbon black, carbon nanotubes, carbon fibers, graphite, wollastonite, magnesium hydroxide, aluminum trihydroxide, attapulgite, titanium dioxide, hydroxyapatite, calcium carbonate, silica, and natural fibers.[1]

Amongst all these composite precursors, those based on clay and layered silicates have been widely investigated probably because the starting clay materials are easily available and because their intercalation chemistry has been studied for a long time.[4–7] They also open the possibility of having nanocomposites, which are a new class of composites, particle-filled polymers for which at least one dimension of the dispersed particles is in the nanometer range.[5–9] Therefore, these nanocomposites exhibit markedly improved mechanical, thermal, optical, and physicochemical properties when compared with the pure polymer.

Among clays, sepiolite has an industrial relevance in Madrid region (there are large deposits) as a raw material, especially owing to its adsorbent properties. Sepiolite is a microcrystalline hydrated magnesium natural silicate with $[(OH_2Mg_8(OH)\cdot 4Si_{12}O_{30}]\cdot 8H_2O$ as the unit cell formula.[10–12] Sepiolite has been employed as reinforcement for inorganic composites,[13] polymeric materials,[14–16] and even for polyolefins, such as polypropylene[17–20] and polyethylene, for which thermal stability and the oxidation induction time are increased with increasing sepiolite content[21]; sepiolite can form a protective layer against theretooxidation on a polyethylene film surface,[22] or even enhance the electrical properties of polymeric insulation,[23] having a significant improvement in mechanical properties.[24]

The intercalation of the polymer (or a monomer subsequently polymerized) inside the galleries leads to a polymer-layered nanocomposite. Several strategies have been considered to prepare polymer-layered

Correspondence to: B. Paredes (beatriz.paredes@urjc.es).

silicate nanocomposites.[5–7] They include two main processes:

1. Solution blended: consists in dispersing the layered silicate within a solution of the polymer followed by either solvent evaporation or polymer precipitation.[25,26]
2. Melt blended: the layered silicate is mixed with the polymer matrix in the molten state. Under these conditions and if the layer surface is sufficiently compatible with the polymer, the polymer can crawl into the interlayer space.[5,27–29]

Traditionally, polymer/clay nanocomposites have been prepared by these two methods. However, one of the key points in nanocomposites is the interaction between nanoparticles and polymer. In the particular case of polyolefins, there is a weak interfacial adhesion between so much different constitutive components due to the hydrophilic character of the clay. Additionally, in these methods the strong interactions between nanoparticles can cause the formation of agglomerates and consequently, the premature breakdown of the material. An option to overcome these problems for obtaining a homogeneous distribution and a good interfacial adhesion between both phases is the chemical modification of the filler surface, turning the hydrophilic clay into a more organophilic material.[30–34]

As alternative strategies, new *in situ* preparation methods have been developed. These methods include the *in situ* polymerization (ISP) and the *in situ* blended (ISB) techniques. In the last one, the polyolefin is blended with the clay during the polymerization stage,[35] whereas the ISP method is based on the intercalative polymerization of the monomer by immobilizing the catalytic system over the clay material.[36–40] The ISP method is also addressed to the large-scale applicability of metallocenes since heterogeneous polymerization conditions are needed in order to ensure good product morphology and avoid reactor fouling.[41–43] Both strategies are based on one-pot synthesis of the polyolefin nanocomposite, a clear advantage over other preparation routes. Moreover, compatibility of clay and polymer matrix, as well as clay dispersion, can be improved.

In this work, ISB together with ISP processes have been employed using MAO/$(nBuCp)_2ZrCl_2$ catalytic system in ethylene polymerization, being sepiolite the clay chosen for the study due to its natural origin and abundance in Spain. Moreover, as it is desirable to get polyethylene particles with a defined morphology, commercial polymerization silica was used as support and compared with sepiolite.

Apart from the goal of making a comparison between both *in situ* processes and obtaining materials with improved mechanical properties due to the clay presence, the main aim of this work involves the development of a new method as a combination of the previous ones. The "*in situ* polymerization" method is quite convenient for metallocene systems, as it is mentioned above; however, the amount of clay in the polymer is usually quite low. In that sense, the "*in situ* blended" method allows achieving bigger clay loadings in the polymer and it is easy to prepare a composite with given clay loading, but in this method there are the problems related with an homogeneous catalytic system. Therefore, the necessity of our work is the combination of both methods since it is possible to overcome the problems that each of them shows when employing individually.

This combined method has been also applied to the synthesis of linear low-density polyethylene (LLDPE), which has a great industrial interest for its applications in packaging, films, cable coatings, etc.[44,45] although, in some cases, its use is limited by their drawbacks such as low mechanical strength, low thermal resistance, and poor optical properties[46]; thus, in order to improve the specific properties of these polymers, the addition of some fillers is necessary.[47,48]

EXPERIMENTAL

Polymerization reactions

Sepiolite supplied by Tolsa S.A. (Madrid, Spain) was employed as filler. Prior use it was treated at 200°C for 5 h. Heterogeneous catalysts called ISP and REF were prepared by impregnating sepiolite or silica (Grace Sylopol 2104, Maryland, USA), respectively, with a mixture containing a solution of methylaluminoxane (MAO 30 wt % in toluene, Witco Illinois, USA) and a solution of bis(butylcyclopentadienyl)zirconium dichloride ($(nBuCp)_2ZrCl_2$, 97% Aldrich Schnelldorf, Germany) in dry toluene under inert nitrogen atmosphere using Schlenk technique and a glove box. The catalyst supported on silica (REF) was used as a reference because it is the most common support for metallocene systems.[43] The amounts of MAO and metallocene were calculated in order to get supported catalysts with an Al(MAO)/Zr molar ratio of 190, according to previous studies.[49] The impregnations were performed at room temperature, in a stirred vessel for 3 h with a volume of impregnating solution thrice the pore volume of the support. Then, the solids were dried under nitrogen flow and stored in glove box.

Ethylene polymerizations were performed in a 1-L stirred-glass reactor using heptane as solvent, at 70°C. A mass-flow indicator allows to measure ethylene flow rate consumption in order to keep the reactor pressure at 5 bar during the polymerization. After 30 min, polymerization reaction was stopped by depressurization and quenched by addition of acidified (HCl) methanol. The polyethylene obtained

was separated by filtration and dried. If the catalytic system was supported on silica or sepiolite, tri-isobutylaluminum (TIBA, 30 wt % in heptane, Witco Illinois, USA) was also added acting as scavenger in an Al(TIBA)/Zr molar ratio of 400, while for the homogeneous catalytic system an Al(MAO)/Zr molar ratio of 10,000 was used.

Polyethylene samples were obtained by different routes:

(a). ISP method, using supported catalysts ISP and REF.
(b). ISB polyethylene/clay (ISB) using the homogeneous catalytic system and adding 1 g of sepiolite clay to the reactor at the beginning of the polymerization.
(c). A new method combining both explained methods (ISB+ISP), that is, using the catalytic system supported on clay or silica and adding 1 g of sepiolite before the polymerization started.
(d). ISB+ISP method using two different loadings of 1-hexene before the ethylene polymerization is started.

Characterization

Thermogravimetric analyses (TGA) of sepiolite and polyethylene samples (to calculate clay loading from the constant mass observed at 600°C) were carried out in a SDT 2960 TA Instrument heating the sample up to 600°C with a rate of 5 °C/min under dry air. Morphology and structure of the materials were observed by transmission electron microscopy (TEM) taken on a Phillips TECNAI 20 microscope with an accelerating voltage of 200 kV and scanning electron micrographs (SEM), taken on a Phillips XL30 ESEM (environmental scanning electron microscope) equipped with a tungsten filament and an accelerating voltage of 15 kV.

Textural properties of silica, sepiolite, and supported catalysts were determined by N_2 adsorption–desorption isotherms at 77 K, obtained by means of a Micromeritics TRISTAR 2050 sorptometer. Prior to the adsorption, the samples were outgassed under vacuum at 200°C for 2 h. X-ray powder diffraction (XRD) data were acquired on a Philips X'PERT MPD diffractometer using Cu Kα radiation within the $2\theta \sim 0.5°$–$50°$ range using a step size of 0.04°.

Molecular weight and molecular weight distributions were determined with a Waters ALLIANCE GPCV 2000 gel permeation chromatograph (GPC) equipped with viscosimetrical detector, and three Styragel HT type columns (HT3, HT4 and HT6) with exclusion limit 1×10^7 for polystyrene. Polymer melting points (T_m), crystallization temperatures (T_c), and crystallinities were determined in a METTLER TOLEDO DSC822 differential scanning calorimeter (DSC), at a heating rate of 10 °C/min in the temperature range 23–160°C. The heating cycle was performed twice, but only the results of the second scan are reported.

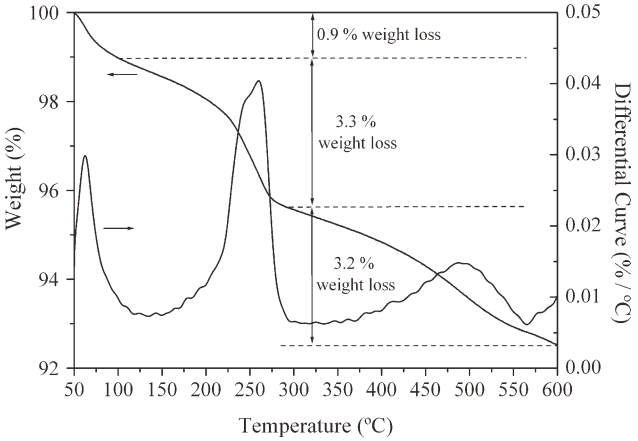

Figure 1 Thermogravimetric and differential thermogravimetric curve for the controlled rate thermal analysis of sepiolite.

A Mercury Plus 400 MHz was used to characterize copolymers by ^{13}C-NMR measurement and determined their 1-hexene molar fraction. Spectra were obtained with a coaxial 10-mm QNP probe with 1,2,4-trichlorobenzene and 1,1,2,2-tetrachloroethylane-d_2. Polymer samples were examined as 10–15% (w/v) solutions with 10 s pulse repetition and 1024 scans.

Dynamic mechanical analysis (DMA) was carried out with a DMA Q800 V 7.1 Build 116 from T. A. Instruments at fixed frequency (1 Hz) with a heating rate of 2 °C/min between −30 and 160°C, the sample dimensions between the clamps were $40 \times 13 \times 2$ mm^3.

The morphologies and dispersion of the clay layers in the composites were examined by XRD and TEM in an ultra-thin slide obtained from the melted plates by sectioning with a glass and diamond blade in a cryogenic-ultramicrotome (Leica EM FC6).

RESULTS AND DISCUSSION

Clay and catalysts characterization

As explained in the introduction section, sepiolite is a naturally hydrated magnesium silicate belonging to the clay mineral family (specifically, to the group of crystalline minerals with chain structure).[10,11] The unit cell formula $[(OH_2Mg_8(OH)\cdot 4Si_{12}O_{30}]\cdot 8H_2O$,[12,50] indicates two types of water molecules, magnesium coordinated and adsorbed water, which can be observed in the TGA and DTA curves shown in Figure 1. Three distinct weight losses can be observed: the first step occurs at 60°C and is attributed to the loss of adsorbed water, the second step is observed at 260°C and corresponds to the loss of hydration water and, finally, the third step is complex and a

TABLE I
Textural Properties of Sepiolite, Silica, and Supported Catalysts

	BET surface area (m^2/g)	Pore volume (cm^3/g)
Sepiolite	218	0.30
MAO/$(nBuCp)_2ZrCl_2$/ Sepiolite	90	0.073
Silica	276	1.81
MAO/$(nBuCp)_2ZrCl_2$/ Silica	245	1.36

broad DTA peak is observed between 370 and 560°C, which is related with the loss of magnesium coordinated water molecules.[50,51]

Table I shows textural properties of sepiolite, silica, and supported catalysts. Because of MAO/metallocene incorporation (14.2 and 13.8 wt % of Al(MAO), 0.25 and 0.24 wt % of Zr, for sepiolite and silica, respectively), the sepiolite surface area and pore volume are greatly reduced, which can be related with some pore blocking.[52]

The XRD powder pattern of sepiolite (Fig. 2) shows the characteristic reflection at $d_{001} = 12.2$ Å ($2\theta = 7.3°$), corresponding to its interlayer distance.[12,53] TEM (Fig. 3) confirms the structural arrangement of sepiolite galleries while SEM, included in this figure, point to an irregular morphology with particle sizes in the 2–10 μm range. In contrast, silica (not shown) consists of particles with well-defined spherical morphology and narrow particle size distribution centered at 56 μm.

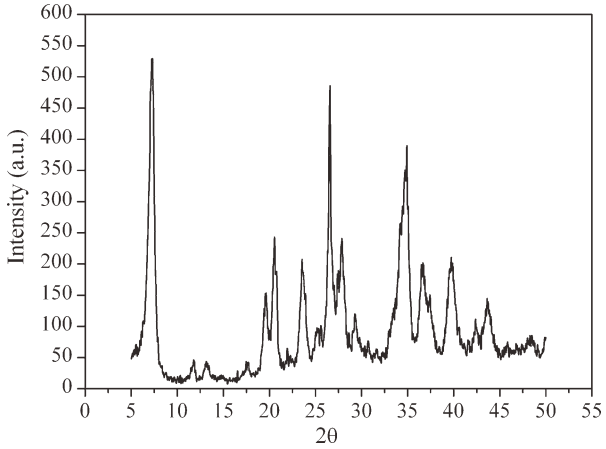

Figure 2 X-ray diffraction pattern of sepiolite.

Figure 4 compares low angle XRD patterns of sepiolite before and after the incorporation of the MAO/metallocene catalytic system. As no change in

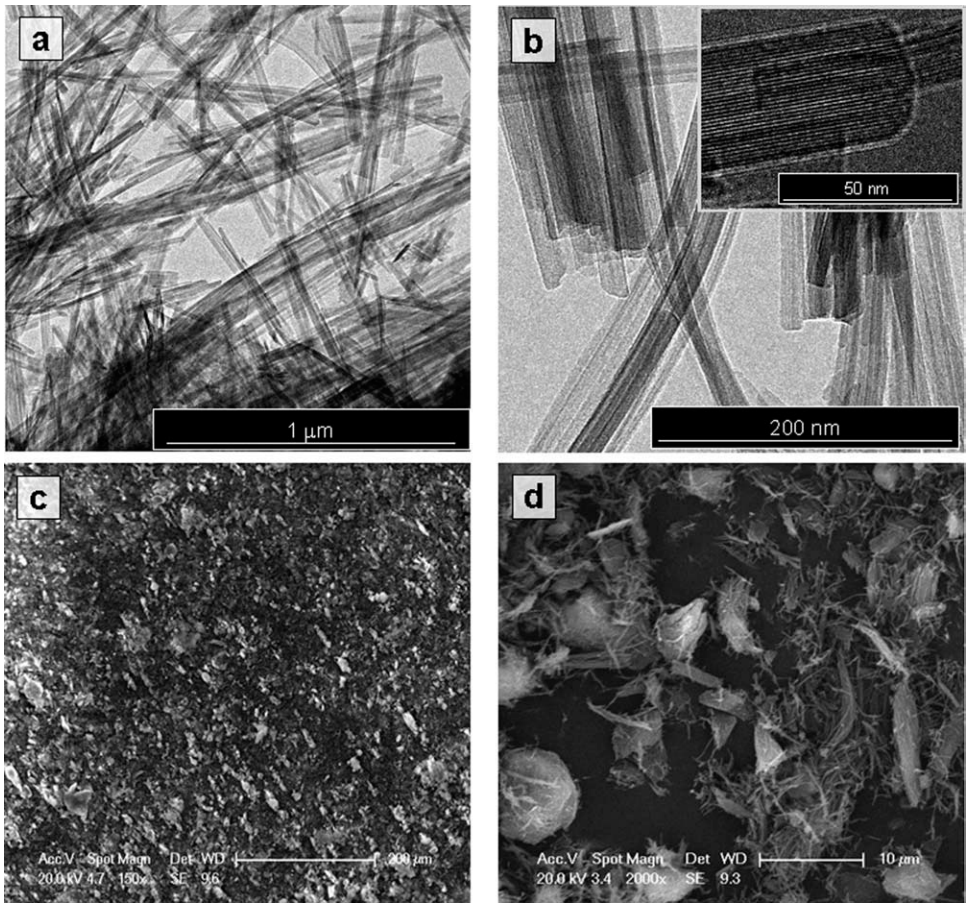

Figure 3 Sepiolite images from (a, b) TEM and (c, d) scanning electron microscopy.

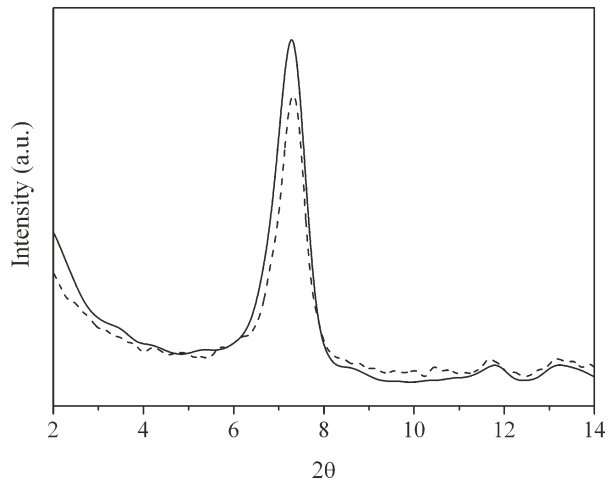

Figure 4 X-ray diffraction patterns of (—) sepiolite and (---) MAO/$(nBuCp)_2ZrCl_2$/sepiolite catalyst.

the diffraction peak is observed, the addition of the MAO/metallocene has not modified the sepiolite interlayer distance. For this reason and taking into account the size of the MAO/metallocene complex,[54] it is probable that the catalytic system will be mainly anchored on the external surface of the sepiolite [Scheme 1(a)], which is in agreement with textural properties of sepiolite after MAO/metallocene anchorage that implies a pore volume reduction of 73%. If the catalytic system would be anchored between layers it had implied an increment in the interlayer distance [Scheme 1(b)] and, therefore a shift in the diffraction peak to lower angles.

Comparison between synthesis methods

As expected, the highest polymerization activity (Table II) is obtained using the homogeneous MAO/metallocene catalytic system (HOMO) and ISB polymerization method (ISB). When the catalytic system is supported on the clay (ISP and ISB+ISP) similar activities are obtained but they are lower than that obtained with the homogeneous catalytic system.[41,42] However, the polymerization activity is even worse if MAO/$(nBuCp)_2ZrCl_2$ is supported on a traditional support like silica (REF and ISB+ISP[REF] samples). According to the literature, this higher activity may be related with a strong interaction between a Lewis acid like MAO with the basic clay's surface.[32,38] Also, it can be related with an easier access to the catalytic centers in the catalyst supported over sepiolite as they seem to be mainly located in the external surface.

TABLE II
Ethylene Polymerization Activity with MAO/$(nBuCp)_2ZrCl_2$ Catalytic System

Polyethylene	Activity (g PE/mol Zr·h·bar)
HOMO	3.56×10^7
ISB	2.65×10^7
ISP [MAO/(nBuCp)$_2$ZrCl$_2$/Sepiolite]	6.05×10^6
ISB+ISP	3.97×10^6
REF [MAO/(nBuCp)$_2$ZrCl$_2$/Silica]	6.20×10^5
ISB+ISP[REF]	8.64×10^5

Time = 30 min; n-heptane = 600 mL, T = 70°C, ethylene pressure = 5 bar.

Polyethylene characterization results are shown in Table III. Polyethylene/sepiolite composites have higher molecular weight and melting temperatures than polyethylene obtained from the homogeneous catalysts or even supported on silica, in spite of low clay loadings as is the case in the ISP sample. The lower molecular weight in the HOMO polymer is

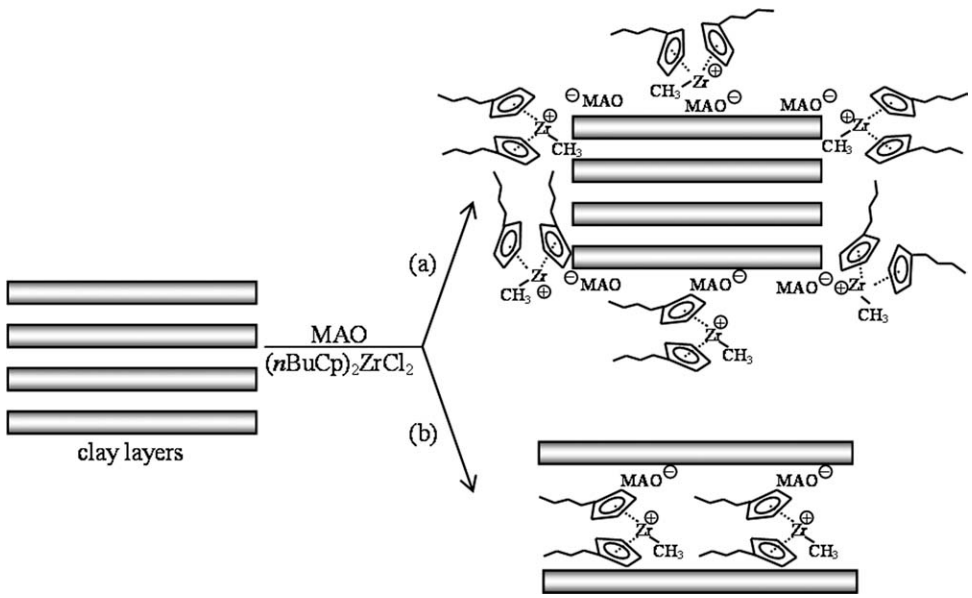

Scheme 1 Inmobilization of MAO/$(nBuCp)_2ZrCl_2$ over sepiolite: (a) external surface and (b) between layers.

TABLE III
Properties of Polyethylene and Polyethylene/Clay Composites

Polyethylene	M_w (g/mol)	M_w/M_n	T_m (°C)	α (%)	Clay (wt %)
HOMO	35,400	2.69	133	62	–
ISB	317,000	2.99	138	65	2.9
ISP	243,000	3.22	137	64	0.2
ISB+ISP	298,000	3.25	138	66	3.8
REF	195,000	3.58	134	62	–
ISB+ISP[REF]	266,000	3.23	135	64	10

due to the higher amount of MAO in the reaction medium (Al(MAO)/Zr = 10,000 against 190 for the heterogeneous catalysts) which favored chain transfer reactions. Zirconocene immobilization prevents deactivation by bimolecular processes increasing molecular weight.[41,42] It is worth mentioning that although the ISB polymerization method implies the incorporation of the homogeneous metallocene catalyst together with 1 g of clay into the polymerization reactor, the properties of ISB polyethylene are close to that corresponding to polyethylene obtained from supported catalytic systems. So, it could be reasonable to propose that before the polymerization reaction is started the MAO/metallocene catalytic system could be adsorbed on the sepiolite surface. The increase in the melting point of the composites materials could be related with a hindered motion of the polymer chain segments by the presence of the clay, thus the crystal growth is retarded.[31] The clay presence also results in an increase in crystallinity, parallel to a higher melting temperature, ascribed to the nucleating activity of the nanofiller which may allow increasing the crystalline fraction of polymer, resulting in improved properties.[31,40] Polydispersity indexes are slightly higher for supported catalysts, which is common in the case of metallocene catalysts due to the generation of different activity sites in the immobilization processes.[42]

The structure of composites analyzed by XRD is shown in Figure 5. No differences were found in the XRD patterns of polymers prepared by ISP, ISB, or the combination of both methods (ISB+ISP, ISB+ISP[REF]). The four samples show the typical polyethylene orthorhombic lattice corresponding to [110] and [200] diffraction peaks at 21.5° and 23.9°, respectively. Besides, the main peak corresponding to the clay is not shifted and, it can be clearly observed in the low angle region. So, the clay interlayer spacing remains unaltered because the polymer is unable to intercalate between the sepiolite sheets. This result agrees with Scheme 1(a) as previously discussed; the interlayer distance is not big enough to accommodate the catalytic system, and it should be placed on the clay external surface area producing ethylene polymerization around clay particles. It has to be mentioned that the signal assigned to the [001] plane in the sepiolite is not observed in the ISP sample because, in this case, the clay is only used as catalyst carrier and the amount of clay in the ISP polyethylene is very low (Table III).

SEM images of polyethylene samples are shown in Figure 6. As it is known, one of the main disadvantages of the metallocene-based polymerization technology lays in the lack of morphology controlling the polymer particle [Fig. 6(a)], and reactor fouling when these catalysts are used in homogeneous processes.[41–43] This features, together with others, as the high Al/metallocene ratios required, justifies the imperative need of the metallocenes heterogeneization process. So, SEM images of ISB, ISP, REF, ISP+ISB, and ISP+ISB[REF] polyethylenes show independent particles typical of heterogeneous polymerization reactions. In this sense, it is important to underline that although the ISB polymerization method uses the catalytic system in homogeneous phase, the obtained PE particles have the same morphology as ISP and ISB+ISP samples. So, as explained before, the homogeneous catalytic system may be adsorbed on the clay surface, acting as a heterogeneous catalyst.

TEM images of ISB, ISB+ISP, and ISB+ISP[REF] polyethylene/clay composites are shown in Figure 7. A uniform dispersion of sepiolite clay in the

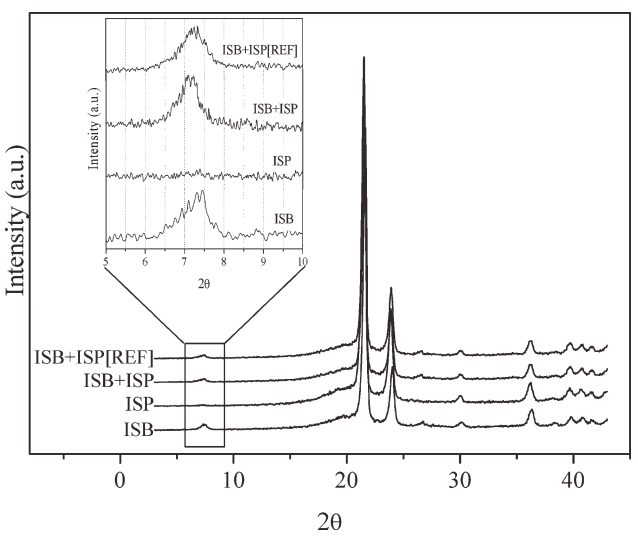

Figure 5 X-ray diffraction patterns of polyethylene/clay composites.

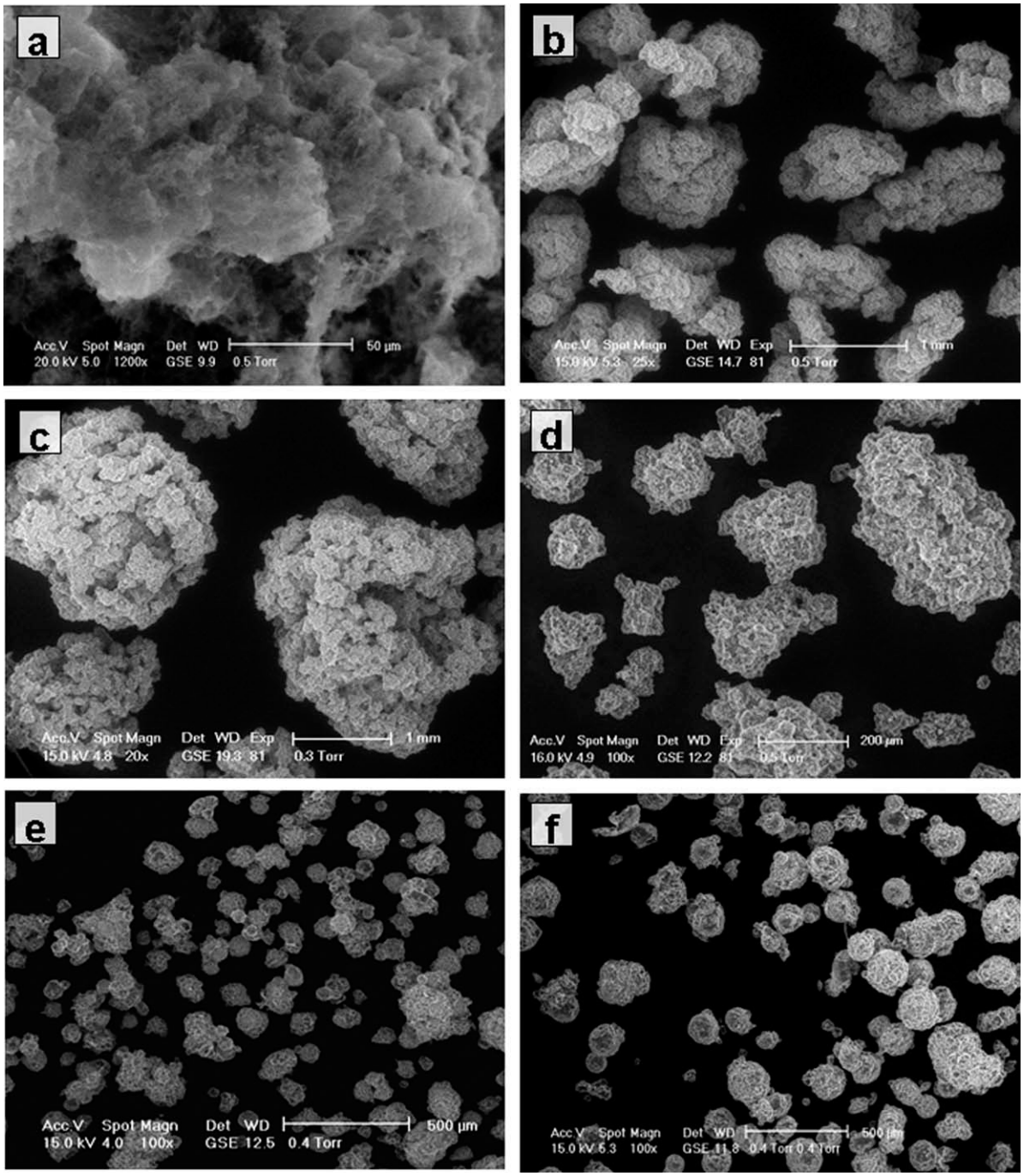

Figure 6 Scanning electron microscopy images of polyethylene samples: (a) HOMO, (b) ISB, (c) ISP, (d) ISB+ISP, (e) REF, and (f) ISB+ISP[REF].

polyethylene matrix can be observed, without any indication of clay aggregation. These results are in agreement with XRD conclusions, indicating that the laminar clay structure is retained and no exfoliation or intercalation took place. Besides, when ISB+ISP sample is studied by back scattered, electron signal (Fig. 8) is possible to detect the clay inserted around the polymer particle surface.

DMA has been used to study temperature dependence of the storage modulus of polyethylene/clay composites. Figure 9 shows higher storage moduli for the materials synthesized in the presence of clay in comparison with HOMO and REF samples, particularly at lower temperatures. This behavior can be explained assuming that the matrix of the composite consist of two parts. One corresponds with the macromolecular chains of polyethylene, where the state of the chains is the same in the pure polyethylene, and the other is the interphase, which is formed by the physical or chemical interaction of

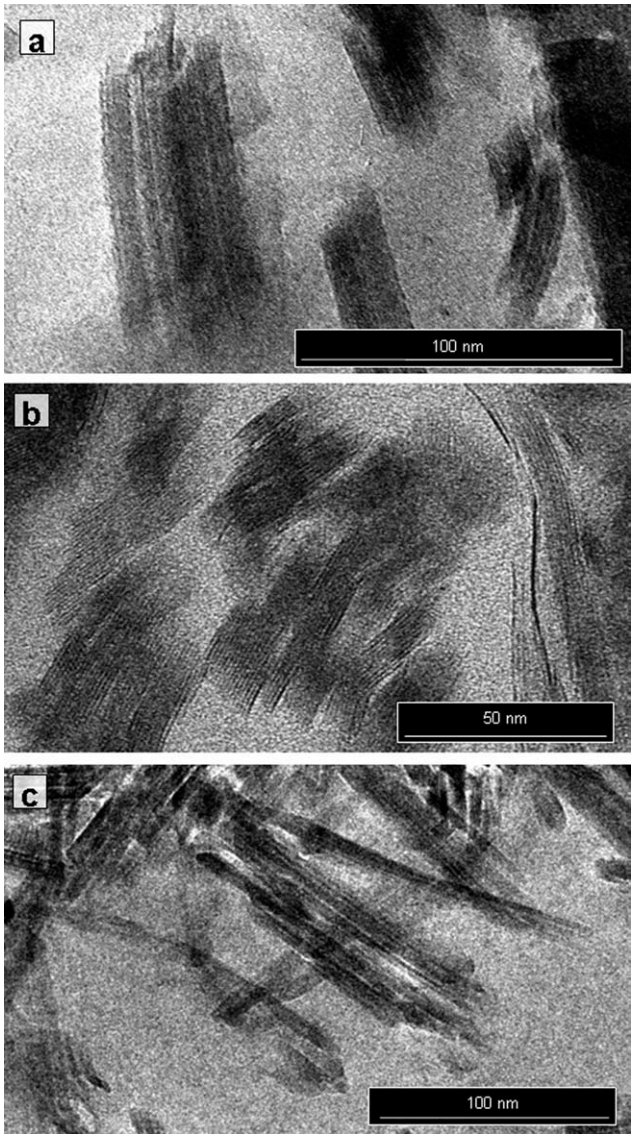

Figure 7 TEM images of polyethylene/clay composites: (a) ISB, (b) ISB+ISP, and (c) ISB+ISP[REF].

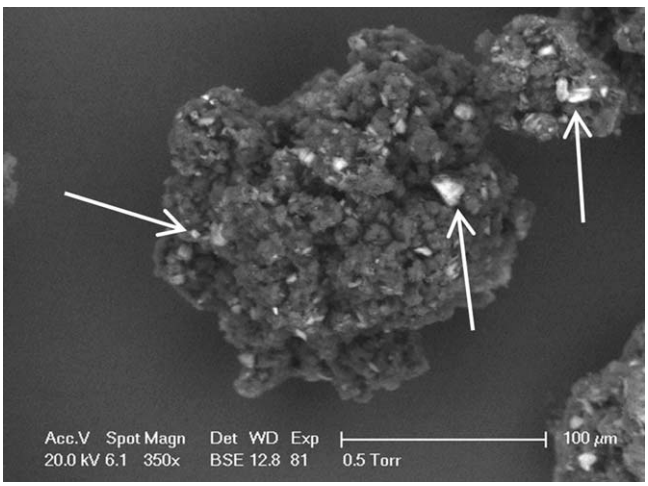

Figure 8 Image of ISB+ISP composite analyzed by back scattered electron (BSE).

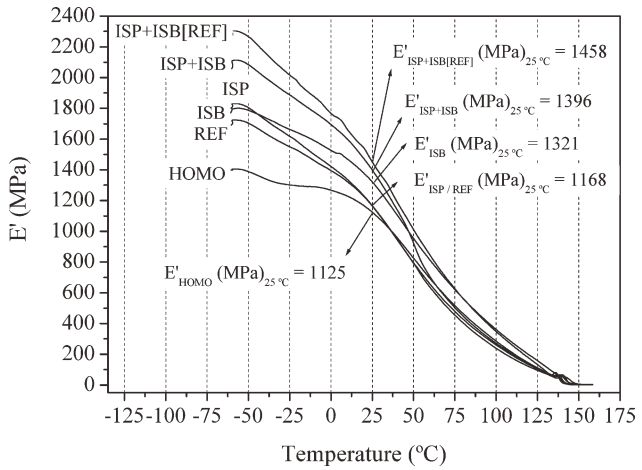

Figure 9 Variation of the storage modulus as a function of the temperature for polyethylene samples.

the polyethylene molecules on the filler's surface. The macromolecular chains of the interphase are restricted to the surface of the filler and, therefore their molecular motion is greatly limited determining the storage modulus.[55] At low temperatures, that motion is even more restricted leading to higher storage modulus in the presence of clay.

Composite with a clay content of 3.8 wt % (ISB+ISP) have a larger interphase area between the matrix and the filler and, therefore a higher storage modulus than ISP and even ISB, so the new combined method is a good approach to obtain polyethylene/clay composites with improved properties. By comparison of the storage modulus values for each sample determined at 25°C shown in Figure 9, it can be seen an increment of 20% for the ISB+ISP[REF] polyethylene compared to the same sample without clay (REF); this is the biggest improvement, which is related also with the biggest clay loading.

Synthesis of LLDPE employing ISB+ISP method

Table IV shows the results of the catalytic activity obtained for the two different employed catalytic systems, over sepiolite (ISB+ISP) and silica (ISB+ISP[REF]), in the presence of 1 g of clay in the reaction medium and different 1-hexene amounts

TABLE IV
Ethylene Polymerization Activity with MAO/ (nBuCp)$_2$ZrCl$_2$ Catalytic System

	Activity (g PE/mol Zr·h·bar)	
1-hex (mol/L)	ISB+ISP	ISB+ISP[REF]
0.066	3.81×10^6	1.51×10^6
0.318	6.34×10^6	3.27×10^6

Time = 30 min; n-heptane = 600 mL, T = 70°C, ethylene pressure = 5 bar.

TABLE V
Properties of LLDPE/Clay Composites

	1-hex (mol %)	M_w (g/mol)	M_w/M_n	T_m (°C)	α (%)	Clay (wt %)
ISB+ISP						
1-hex (mol/L)						
0.066	0.94	224,000	3.14	124	45	3.9
0.318	3.21	206,000	3.38	112	34	2.3
ISB+ISP[REF]						
1-hex (mol/L)						
0.066	0.88	176,000	3.11	122	51	5.9
0.318	3.24	186,000	3.23	108	37	2.8

loaded in the reactor. It is well known that in the copolymerization of ethylene with an α-olefin, the insertion of the comonomer usually affects the catalytic activity. This is the so-called "comonomer effect."[44,56,57] This effect induces changes in the activity depending on the type of comonomer, the polymerization conditions, and the nature of the catalyst. In both cases, ISB+ISP and ISB+ISP[REF], a soft positive comonomer effect is observed, being the activities achieved with the catalytic system supported over sepiolite higher than over silica, as previously discussed.

Table V summarizes polyethylene properties. The incorporation of 1-hexene for all copolymers increases with the amount of comonomer loaded in the reactor. 1-hexene incorporation is not affected by the support that has been used to prepare the supported catalyst. Some authors claim that incorporation of the comonomer is just related to the structure of metallocene catalyst.[58]

Results of crystallinity and melting temperatures obtained by DSC reveal that the incorporation of 1-hexene to the polymer chain involves synthesizing a product with lower crystalline fraction. It can be seen how these values range from 62 to 64% of crystalline fraction in the absence of comonomer, to 34–37% when the comonomer incorporation reaches values close to 3.2 mol %. The larger size of 1-hexene molecule together with the reduction in chain regularity hinders its crystallization. Similarly, when the amount of 1-hexene incorporated increases, melting temperatures decrease due to short-chain branching introduced by 1-hexene as branches avoid crystallization processes.[44–46]

Molecular weight decreases as the incorporation of 1-hexene increases. Comonomer incorporation favors termination reactions,[44] since α-olefins generally act as chain-transfer agents allowing to end a chain but to continue polymerizing the active site. The polydispersity indexes are approximately constant, with values expected for single-site catalysts,[41–43] independent on the comonomer content, clay addition, and the catalytic system used.

Mechanical properties of LLDPE composites were investigated by DMA (Fig. 10), also results without additional clay in the reaction medium are presented as reference. The storage modulus decreases as the 1-hexene content increases as a consequence of the stiffness decrease as the crystallinity is reduced.[55] Mechanical properties of polyethylenes synthesized in the presence of 1 g of clay are improved in comparison to those synthesized without additional

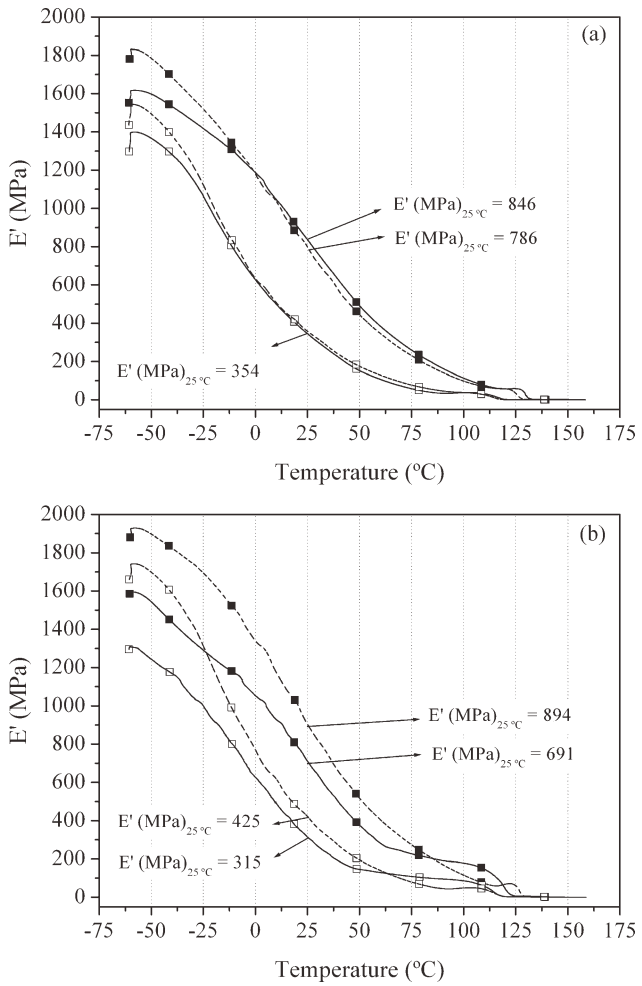

Figure 10 Variation of the storage modulus as a function of the temperature for samples synthesized in presence of 1 g of sepiolite in the reaction medium (---) and without additional clay (–) with (a) ISP and (b) REF; synthesized with 1-hexene loaded in the reactor (mol/L) (■) 0.066 and (□) 0.318.

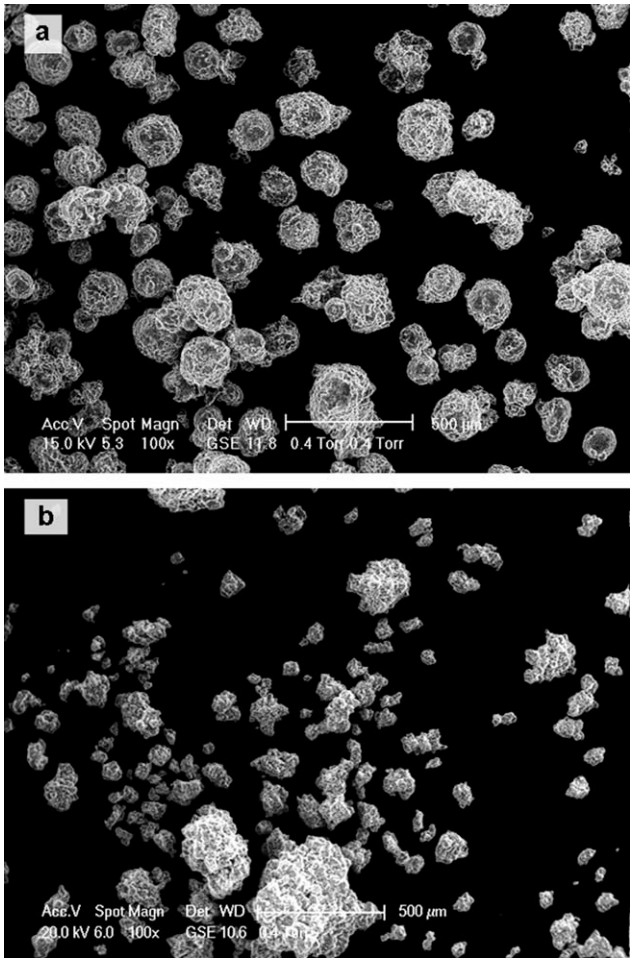

Figure 11 Scanning electron microscopy images of LLDPE/clay (0.066 mol/L of 1-hexene loaded in the reactor) for (a) ISB+ISP[REF] and (b) ISB+ISP composites.

sepiolite which can be seen by an increase of E', more remarkable at lower temperatures, indicating a reinforcement effect of sepiolite. This effect is quite more pronounced when the catalytic system is immobilized over silica than sepiolite. Figure 10 shows the storage modulus values for each sample determined at 25°C; when silica is used as support and 0.318 mol/L of 1-hexene were added into the reactor an increment around 26% of the E' value can be observed with 2.8 wt % of clay. These results remark the importance of the synthesis in the presence of clay, since a LLDPE with improved mechanical properties can be obtained. Moreover, when this LLDPE is synthesized with the catalytic system over silica, the particle morphology is appropriate, granular with high bulk density and very few fine particles [Fig. 11(a)][42,43] based on fragmentation and replica phenomena that take place during polymerization. These phenomena also occur with sepiolite as carrier, but polymer morphology is irregular in shape and size [Fig. 11(b)] as it is the original clay.

CONCLUSIONS

Polyethylene/sepiolite clay composites have been synthesized through ISB, ISP, and a new method combining both (ISB+ISP), employing sepiolite and silica as carriers for MAO/$(n\text{BuCp})_2\text{ZrCl}_2$ catalytic system.

The ISB method gives higher polymerization activities than ISP and ISB+ISP as it is usual when comparing homogeneous to heterogeneous metallocene systems. However, based on polyethylene properties, in the ISB method the catalyst may be adsorbed on the clay surface before starting the polymerization since properties are closer to those obtained with the immobilized catalytic system.

When the catalytic system is supported over the clay, sepiolite keeps its layered structure with no changes in the interlayer distance although its textural properties are greatly reduced; indicating that the catalytic system must be preferably anchored on the external surface and reaction will not take place inside the galleries. This agrees with TEM and XRD of polyethylene/sepiolite composites, where the clay is well dispersed on the polymer matrix but its interlayer spacing remains unaltered, so neither an intercalated nor an exfoliated nanocomposites are formed. Nevertheless, there is an important improvement of the polymerization activity obtained when typical silica support is replaced by sepiolite; this fact points to a strong interaction between a Lewis acid like MAO with the basic clay surface or an easier monomer access to the catalytic centers.

The method developed in this work, ISB+ISP, does not lead to significant differences in catalytic activity in comparison with ISP, either employing sepiolite or silica as supports, but polyethylenes present the highest storage modulus at 25°C, so the new combined method is a good approach to obtain polyethylene/clay composites with improved properties, mainly if silica is employed as carrier, where an increment in the storage modulus of 20% is achieved. The use of this method for the synthesis of LLDPE using silica as catalytic support allows increasing the E' value up to 26% with 2.8 wt % of clay; so it can be obtained a copolymer with combined properties such as low melting temperature and easy processing, good morphology, and high storage modulus.

References

1. Nwabunma, D.; Kyu, T. Polyolefin Composites; Wiley: Hoboken, New Jersey, 2008.
2. Shonaike, G. O.; Advani, S. G. Advanced Polymeric Materials. Structure Property Relationships; CRC Press: Boca Raton, Florida, 2003.
3. Kato, M.; Usuki, A.; Hasegawa, N.; Okamoto, H.; Kawasumi, M. Polym J 2011, 43, 583.

4. Mark, J. E. Polym Eng Sci 1996, 36, 2905.
5. Alexandre, M.; Dubois, P. Mater Sci Eng 2000, R28, 1.
6. Ciardelli, F.; Coiai, S.; Passaglia, E.; Pucci, A.; Ruggeri, G. Polym Int 2008, 57, 805.
7. Okamoto, O. Rapra Rev Rep 2003, 14, 178.
8. Giannelis, E. Adv Chem Ser 1995, 245(Materials Chemistry), 259.
9. Wang, Q.; Zhou, Z.; Song, L.; Xu, H.; Wang, L. J Polym Sci Part A: Polym Chem 2003, 42, 38.
10. Aramendia, M. A.; Borau, V.; Jimenez, C.; Marinas, J. M.; Ruiz, J. R. Solid State Nucl Magn Reson 1997, 8, 251.
11. Aramendia, M. A.; Borau, V.; Corredor, J. I.; Jimenez, C.; Marinas, J. M.; Ruiz, J. R.; Urbano, F. J. J Colloid Interface Sci 2000, 227, 469.
12. Ruiz-Hitzky, E. J Mater Chem 2001, 11, 86.
13. Kavas, T.; Sabah, E.; Celik, M. S. Cem Concr Res 2004, 34, 2135.
14. Zheng, Y.; Zheng, Y. J Appl Polym Sci 2006, 99, 2163.
15. Ekici, S.; Isikver, Y.; Saraydin, D. Polym Bull 2006, 57, 231.
16. Chen, H.; Zheng, M.; Sun, H.; Jia, Q. Mater Sci Eng A 2007, 445–446, 725.
17. Linares, A.; Morales, E.; Ojeda, M. C.; Acosta, J. L. Macromol Mater Eng 2003, 147, 41.
18. Ma, J.; Bilotti, E.; Peijs, T.; Darr, J. A. Eur Polym J 2007, 43, 4931.
19. Tartaglione, G.; Tabuani, D.; Camino, G.; Moisio, M. Compos Sci Technol 2008, 68, 451.
20. Rodriguez-Llamazares, S., Rivas, B. L.; Perez, M.; Perrin-Sarazin, F.; Maldonado, A.; Venegas, C. J Appl Polym Sci 2011, 122, 2013.
21. Gul, R.; Islam, A.; Yasin, T.; Mir, S. J Appl Polym Sci 2011, 121, 2772.
22. Garcia, N.; Hoyos, M.; Guzman, J.; Tiemblo, P. Polym Degrad Stab 2009, 94, 39.
23. Guastavino, F.; Dardano, A.; Squarcia, S.; Tiemblo, P.; Guzman, J.; Benito, E.; Garcia, N. Annu Report—Conference on Electrical Insulation and Dielectric Phenomena Virginia, USA 2009; p 592.
24. Arroyo, M.; Perez, F.; Vigo, J. P. J Appl Polym Sci 2003, 32, 5105.
25. Ogata, N.; Jimenez, G.; Kawai, H.; Ogihara, T. J Polym Sci Part B: Polym Phys 1997, 35, 389.
26. Ogata, N.; Kawakage, S.; Ogihara, T. J Appl Polym Sci 1997, 66, 573.
27. Ding, P.; Qu, B. J Polym Sci Part B: Polym Phys 2006, 44, 3165.
28. Heinemann, J.; Reichert, P.; Thomann, R.; Mulhaupt, R. Macromol Rapid Commun 1999, 20, 423.
29. Moncada, E.; Quijada, R.; Retuert, J. J Appl Polym Sci 2007, 103, 698.
30. Park, C. I.; Park, O. O.; Lim, J. G.; Kim, H. J. Polymer 2001, 42, 7465.
31. Shin, S. Y. A.; Simon, L. C.; Soares, J. B. P.; Scholz, G. Polymer 2003, 44, 5317.
32. Xalter, R.; Halbach, T. S.; Muelhaupt, R. Macromol Symp 2006, 236(Olefin Polymerization), 145.
33. Gaboune, A.; Ray, S. S.; Ait-Kadi, A.; Riedl, B.; Bousmina, M. J Nanosci Nanotechnol 2006, 6, 530.
34. He, F. A.; Zhang, L. M.; Jiang, H. L.; Chen, L. S.; Wu, Q.; Wang, H. H. Compos Sci Technol 2007, 67, 1727.
35. Kuo, S. W.; Huang, W. J.; Huang, S. B.; Kao, H. C.; Chang, F. C. Polymer 2003, 44, 7709.
36. Tudor, J.; Willington, L.; O'Hare, D.; Royan, B. Chem Commun 1996, 17, 2031.
37. Dubois, P.; Alexandre, M.; Hindryckx, F.; Jerome, R. J Macromol Sci Rev Macromol Chem Phys 1998, C38, 511.
38. Alexandre, M.; Martin, E.; Dubois, P.; Garcia-Marti, M.; Jerome, R. Macromol Rapid Commun 2000, 21, 931.
39. Weiss, K.; Wirth-Pfeifer, C.; Hofmann, M.; Botzenhardt, S.; Lang, H.; Bruning, K.; Meichel, E. J Mol Catal A: Chem 2002, 143.
40. Alexandre, M.; Dubois, P.; Sun, T.; Garces, J. M.; Jerome, R. Polymer 2002, 43, 2123.
41. Ribeiro, M. R.; Deffieux, A.; Portela, M. F. Ind Eng Chem Res 1997, 36, 1224.
42. Hlatky, G. G. Coord Chem Rev 2000, 199, 235.
43. Severn, J. R.; Chadwick, J. C.; Duchateau, R.; Friederichs, N. Chem Rev 2005, 105, 4073.
44. Galland, G. B.; Seferin, M.; Mauler, R. S.; dos Santos, J. H. Z. Polym Int 1999, 48, 660.
45. Simanke, A. G.; Galland, G. B.; Neto, R. B.; Quijada, R.; Mauler, R. S. J Appl Polym Sci 1999, 74, 1194.
46. Krentsel, B. A.; Kissin, Y. V.; Kleiner, V. I.; Stotskaya, L. L. Polymers and Copolymers of Higher α-Olefins: Chemistry, Technology, Applications; Hanser Publishers: Munich, 1997.
47. Owpradit, W.; Jongsomjit, B. Mater Chem Phys 2008, 112, 954.
48. Desharun, C.; Jongsomjit, B.; Praserthdam, P. Catal Commun 2008, 9, 522.
49. Carrero, A.; van Grieken, R.; Paredes, B. J Appl Polym Sci 2011, 120, 599.
50. Frost, R. L.; Ding, Z. Thermochim Acta 2003, 397, 119.
51. Ovarlez, S.; Chaze, A. M.; Giulieri, F.; Delamare, F. C R Chim 2006, 9, 124.
52. Aznar, A.; Gutierrez, E.; Diaz, P.; Alvarez, A.; Poncelet, G. Microporous Mater 1996, 6, 105.
53. Guengoer, N.; Isci, S.; Guenister, E.; Mista, W.; Teterycz, H.; Klimkiewicz, R. Appl Clay Sci 2006, 32, 291.
54. Babushkin, D. E.; Brintzinger, H. H. J Am Chem Soc 2002, 124, 12869.
55. Kontou, E.; Niaounakis, M. Polymer 2006, 47, 1267.
56. Chien, J. C. W.; Nozaki, T. J Polym Sci Part A: Polym Chem 1993, 31, 227.
57. Koivumaki, J.; Seppala, J. V. Macromolecules 1993, 26, 5535.
58. Fischer, D.; Jungling, S.; Schneider, M. J.; Suhm, J.; Mulhaupt, R. Metallocene-Based Polyolefins, John Wiley & Sons: Chichester, 2000; Vol.1, p 103.